



Published in final edited form as:

*Nanomedicine*. 2017 April ; 13(3): 1235–1243. doi:10.1016/j.nano.2016.11.014.

## Enhanced Efficacy of Combination Heat Shock Targeted Polymer Therapeutics with High Intensity Focused Ultrasound

Nick Frazier<sup>†,‡</sup>, Allison Payne , Christopher Dillon , Nithya Subrahmanyam<sup>‡,§</sup>, and Hamidreza Ghandehari<sup>†,‡,§,\*</sup>

<sup>†</sup>Department of Bioengineering, University of Utah, Salt Lake City, UT 84112, USA

<sup>‡</sup>Center for Nanomedicine, Nano Institute of Utah, University of Utah, Salt Lake City, UT 84112, USA

Department of Radiology and Imaging Sciences, University of Utah, Salt Lake City, UT 84112, USA

<sup>§</sup>Department of Pharmaceutics and Pharmaceutical Chemistry, University of Utah, Salt Lake City, UT 84112, USA

### Abstract

Combination of polymer therapeutics and hyperthermia has been shown to enhance accumulation in selectively heated tumor tissue. The additional use of heat shock (HS)-targeting towards tumor tissues can further enhance accumulation and retention, and improve therapeutic outcomes. In this work, high intensity focused ultrasound (HIFU) was used to generate hyperthermia in prostate tumor tissue. Upregulation of the cell surface HS receptor glucose regulated protein 78 kDa (GRP78) was observed after treatment with HIFU hyperthermia which was then targeted by specific HS-targeting peptides. We used the peptide sequence WDLAWMFRLPVG attached to the side chains of water-soluble *N*-(2-hydroxypropyl)methacrylamide (HPMA) copolymers containing docetaxel (DOC) conjugated via a lysosomally degradable linker. It was shown that HIFU-mediated HS-targeted copolymer-DOC conjugates improved treatment efficacy in a murine prostate tumor xenograft model. These results show that the use of HIFU hyperthermia in combination with HS-targeted polymer-drug conjugates has potential to improve therapeutic outcomes in prostate cancer treatment.

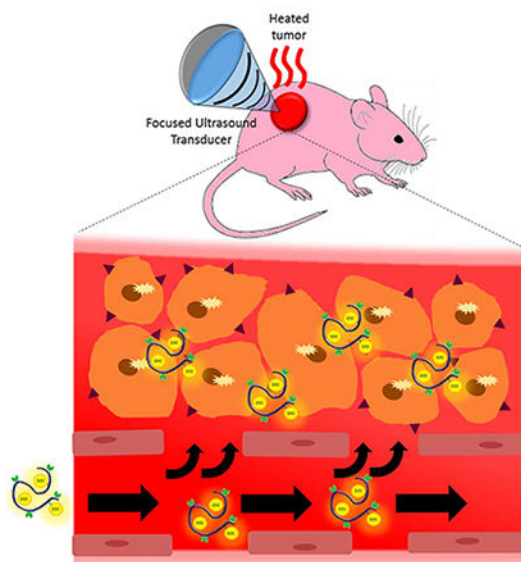
### GRAPHICAL ABSTRACT

The combination of HIFU hyperthermia with heat shock-targeted HPMA-Docetaxel copolymers is used to enhance the delivery and efficacy of these targeted macromolecules.

\*Corresponding author. hamid.ghandehari@pharm.utah.edu, Ph: 801-587-1566, Fax: 801-581-6321, Address: 36 S. Wasatch Dr., Salt Lake City, UT 84112-5001.

Conflict of interest: Authors declare no conflict of interest.

**Publisher's Disclaimer:** This is a PDF file of an unedited manuscript that has been accepted for publication. As a service to our customers we are providing this early version of the manuscript. The manuscript will undergo copyediting, typesetting, and review of the resulting proof before it is published in its final citable form. Please note that during the production process errors may be discovered which could affect the content, and all legal disclaimers that apply to the journal pertain.



## Keywords

High intensity focused ultrasound; hyperthermia; drug delivery; magnetic resonance imaging; prostate cancer

## 1. Background

The ultimate goal of targeted drug delivery is to selectively deliver therapeutics to the disease site and allow for increased dosages to be administered to the patient while simultaneously reducing off-target effects. Polymer therapeutics have been developed in an attempt to accomplish this goal for delivery of anticancer drugs to solid tumors<sup>1</sup>. Such constructs can extend blood circulation times of conventional drugs and increase accumulation within cancerous tissues through passive delivery by the enhanced permeability and retention (EPR) effect<sup>2</sup>. The use of these and other nanomedicines has led to improved therapeutic outcomes with altered biodistribution in certain cases minimizing side effects (e.g. Doxil reducing the cardiotoxicity of doxorubicin)<sup>3</sup>. Still, in a majority of cases only moderately enhanced localization to the tumor tissue is observed, increasing from approximately 1% to 5% of injected dose (ID)<sup>4</sup>. The impact of nanoscale delivery systems for treatment of solid tumors can be limited due to the variability of EPR effect depending on tumor type, size, location, and preclinical to clinical correlation<sup>5</sup>. Therefore, combination approaches must be considered including augmentation of the EPR effect<sup>6</sup>.

Methods to further enhance the delivery of nanomedicines through augmentation of the EPR effect include mild hyperthermia. At the tissue level, this mechanism can both increase blood flow and improve vascular permeability by vasodilation<sup>7</sup> leading to improvements in local delivery. Mild hyperthermia (41-43°C) has been shown to enhance the delivery of nanomedicines to solid tumors<sup>8</sup>. At the cellular level, mild hyperthermia has the ability to upregulate cell surface HS receptor glucose regulated protein 78 (GRP78)<sup>9</sup>. Specific peptide sequences have been developed by phage display which show a strong binding affinity

towards the GRP78 receptors<sup>10</sup>. These peptides include WDLAWMFRLPVG (single letter amino acid abbreviations are used)<sup>11</sup>. Methods such as plasmonic photothermal therapy (PPTT), magnetic fluid hyperthermia (MFH), and radiofrequency ablation (RFA) can induce hyperthermic conditions<sup>8</sup>. We have previously demonstrated that mild hyperthermia by gold nanorod (GNR)-mediated PPTT enhances the delivery of *N*-(2-hydroxypropyl)methacrylamide (HPMA) copolymer-drug conjugates containing GRP78 targeting moieties in the side chains to solid tumors<sup>9</sup>. HS-targeted copolymer-docetaxel (DOC) conjugates showed enhanced efficacy when hyperthermia was applied in combination<sup>11</sup>. While results of this research are promising, PPTT in combination with polymer therapeutics requires a prior injection of nanoparticles delivered intravenously which then accumulate in tumor tissue by the EPR effect<sup>12</sup>. The accumulation of these particles in tumor tissue allows for laser energy to be locally absorbed<sup>13</sup>. However, after this injection, only a small fraction of the gold nanoparticles reach the tumor site leading to a large amount (>90%) of off-target accumulation in other organs such as the liver and spleen<sup>12</sup>. Additionally, in order to heat deep-seeded tumors, an optical fiber needs to be invasively placed in the body. These drawbacks limit the applications of this promising combination strategy. Alternative methods that are non-invasive and provide a higher depth of tissue penetration are needed to improve the clinical application of combination of mild hyperthermia and polymer therapeutics to treat solid tumors.

High intensity focused ultrasound (HIFU) is a non-invasive technique that can locally heat tissues and achieve a large penetration depth of up to approximately 20 cm through the tissue<sup>14</sup>. We have previously shown in pre-clinical mouse tumor models that MRI guided HIFU (MRgHIFU) can be used to non-invasively generate and maintain uniform hyperthermia in subcutaneous tumor tissue and that the resulting thermal effects can lead to enhanced delivery of HPMA copolymer-gadolinium conjugates in solid tumors<sup>15</sup>. It was shown that after 5 hours post heating a significant increase in copolymer accumulation is achieved in heated tumors versus control non-heated tumors. The accumulation of these non-targeted systems enabled a transient increase in copolymer concentration in a mouse sarcoma model peaking at approximately 4-5 hours post HIFU heating<sup>15</sup> as assessed by the longitudinal relaxation time (T1) measured in the tumor tissue and compared to the control tumor. To further build on the utility of HIFU mild hyperthermia in enhancing the delivery of macromolecular constructs, in this manuscript we have used a combination of non-invasive MRgHIFU hyperthermia with HPMA copolymer-WDLAWMFRLPVG conjugates containing docetaxel (DOC) in the side chains to improve the efficacy of the conjugates in a murine model of human prostate xenografts.

## 2. Methods

### 2.1 Synthesis and characterization of HPMA copolymer conjugates

Comonomers of HPMA<sup>16</sup>, *N*-methacryloylglycylglycyl-2-thiazolidine-2-thione (MA-GG-TT), and *N*-methacryloyl-glycylphenylalanylleucylglycine-docetaxel (MA-GFLG-DOC)<sup>17</sup> were synthesized as described previously. DOC was provided by AK Scientific (Mountain View, CA). Free radical precipitation copolymerization using azobisisobutyronitrile (AIBN) as the initiator in methanol at 50°C for 24 hours was used to prepare the copolymers. The

product was then precipitated and washed with diethyl ether followed by dialysis against deionized water to remove unreacted comonomers and initiator. The copolymers were lyophilized to obtain the final product. Weight average molecular weight ( $M_w$ ), number average molecular weight ( $M_n$ ), and polydispersity index (PDI) is calculated by the ratio of  $M_w/M_n$  and were estimated by size exclusion chromatography (SEC).

The GRP78 targeting peptide WDLAWMFRLPVG and corresponding scrambled peptide RWLWVADPFLMG were synthesized via Fmoc chemistry using a Protein Technologies (Tuscon, AZ) PS3 solid phase peptide synthesizer, verified by amino acid analysis and electrospray ionization mass spectrometry (ESI/MS).

## 2.2 Cell culture

The DU145 human prostate cancer cell line was obtained from ATCC (Manassas, VA) and cultured at 37 °C in a humidified atmosphere of 5% CO<sub>2</sub> in Eagle's Minimum Essential Medium supplemented with 10% fetal bovine serum (FBS). Cells were maintained in a logarithmic growth phase during all studies.

## 2.3 In vitro efficacy of heat shock targeted copolymer-drug conjugates

DU145 cells (3000 per well) were plated in 96-well plates for 24 h. Media was then removed and replaced with media containing treatments. Cells were exposed to either heat shock targeted copolymers or untargeted copolymers for 12 hours at varying concentrations between 0 and 1200 nM DOC concentration. One group was incubated at 37°C while a second group was exposed to heat shock (HS) (43°C for 30 minutes) and then incubated at 37°C for the remainder of the 12 hours. This thermal dose profile was chosen to be consistent with previous experiments<sup>11</sup> as this thermal treatment showed a 4-fold increase in cell receptors *in vitro*<sup>9</sup>. For each treatment case, drug concentrations were varied to include data points ranging from approximately 100% to 0% cell viability. Following drug treatment, media was removed, cells washed with PBS, growth media replaced, and cells were allowed to grow for an additional 60 hours (72 hours of total experiment duration). Media was then removed and cell viability was quantified via CCK-8 assay using a SpectraMax M2 microplate UV spectrophotometer (Molecular Devices, Sunnyvale, CA). Each experiment was performed in triplicate, comprising assessment of viability at 10 different drug concentrations with 4 samples analyzed per concentration. Relative viability was calculated by normalization of UV absorbance against untreated cells. Relative viability as a function of log drug concentration was plotted and non-linear least-squares regression analysis and calculation of inhibitory concentration of 50% (IC<sub>50</sub>) values were performed using GraphPad Prism.

## 2.4 In vivo tumor model

*In vivo* experiments were carried out using nu/nu mice containing two DU145 human prostate cancer subcutaneous tumor xenografts, one on each flank. Inoculations were performed by injecting 200 μL of phosphate buffered solution (PBS) containing 10×10<sup>6</sup> cells subcutaneously and allowing tumors to grow for 28-30 days to reach a size of 7-11 mm in diameter. Tumor sizes were measured every 3 days using calipers. Once the tumors reached the desired size, they were then treated with MRgHIFU hyperthermia.

## 2.5 In vivo MRgHIFU heating

Prior to MRgHIFU treatment, the mice were anesthetized (2% isoflurane), a needle thermocouple was inserted into the center of the tumor and two minutes of temperature data were obtained to determine a baseline tumor temperature. The animal was placed on an agar mold on the MRgHIFU device with the tumor placed in an access hole that provided an acoustic window between the HIFU transducer and the tumor. The agar mold provided a large region to obtain stable MRI phase measurements to improve the MRI temperature measurement reconstruction. A custom two-channel radiofrequency coil was placed on top of the animal, and a small animal monitoring system was used to monitor the animal (respiration and temperature, SA Instruments, Inc.).

All heating was performed using a MRgHIFU small animal system (Image Guided Therapy, Inc., Bordeaux, France, 16-element annular transducer,  $f = 3\text{MHz}$ ,  $1 \times 1 \times 3\text{ mm}$  full-width-half-maximum intensity focal spot size,  $3.5\text{ cm}$  focal length) placed in a Siemens 3T Trio MRI scanner. MR temperatures were monitored with the proton resonance frequency (PRF) method using a 2D segmented-echo planar imaging sequence (TR/TE = 150/13 ms, echo train length = 9, 1.2 s acquisition time,  $2 \times 2 \times 3\text{ mm}$  resolution, 3 slices). Because the phased-array transducer has an annular element design, in-plane focal spot motion was achieved by physically moving the transducer using piezoelectric motors. The experimental setup is shown in axial (Fig 1A) and coronal (Fig 1B) orientations in Figure 1. Susceptibility effects due to ultrasound transducer motion were mitigated using an atlas-based reconstruction<sup>18</sup> where approximately 50 baseline library images were acquired with the transducer moving along the pre-defined trajectory (Fig 1C) multiple times without firing the ultrasound. During sonication, the current MR phase measurement was subtracted from the baseline library phase image that was most similar in a least squared difference sense. Using a previously described MRgHIFU controller<sup>15</sup>, the maximum and mean temperatures in the tumor were monitored and a power range between 3.3 and 5.6 acoustic W was implemented (approximately 3.5 to 4.6 MPa in water) to achieve and maintain an approximate maximum temperature of  $43^\circ\text{C}$ . Using the real-time MR temperature measurements, the MRgHIFU operator was able to adjust the ultrasound power output in real-time using a user interface written in MATLAB. A target maximum temperature of  $43^\circ\text{C}$  was selected to induce mild hyperthermia but not ablation. During post-processing, temperatures were temporally filtered for respiratory artifacts using a low pass digital filter.

## 2.7 In vivo expression of GRP78 with MRgHIFU hyperthermia

MRgHIFU was used to treat one tumor of nu/nu mice bearing two subcutaneous DU145 tumors. The second tumor was left untreated and used as an internal control. MRgHIFU hyperthermia was used to induce HS and determine the upregulation of GRP78 receptors in the heated tumor versus the control tumor. For this experiment, three mice were used to demonstrate the reproducibility of this phenomenon. Eight hours following induction of heat shock, the mice were sacrificed and both tumors were removed and fixed in 10% buffered formalin. Immunohistochemical analysis of GRP78 expression was then performed on paraffin embedded tumor tissue sliced into 4-micron thick sections and stained using a goat polyclonal anti-GRP78 antibody (Santa Cruz Biotechnology, Santa Cruz, CA).

## 2.8 In vivo efficacy of heat shock targeted HPMA copolymer-DOC conjugates with MRgHIFU

The combination of HS-targeted copolymer-drug conjugates and MRgHIFU were evaluated *in vivo* using nu/nu mice bearing two subcutaneous DU145 human prostate cancer tumors. Four treatment groups were studied, each comprised of six mice. Prior to treatment with MRgHIFU hyperthermia to one tumor, one of the four treatments were administered intravenously being either saline, free DOC (formulated in polysorbate 80:EtOH:saline [20:13:67, v/v/v]), untargeted (scrambled peptide) polymer-DOC, or HS-targeted polymer-DOC at 10 mg/kg equivalent of DOC. The mice in each treatment group were monitored over 30 days, twice a week for changes in tumor volume and animal weight. Tumor dimensions (length and width) were measured and tumor volume estimated as length  $\times$  width  $\times$   $\pi/6$ . Normalized tumor volume (mean  $\pm$  STD) and changes in animal weight (mean  $\pm$  STD) are reported as a function of time. After the 30-day study was completed, tumors and organs were removed, fixed in 10% buffered formalin, paraffin embedded, sectioned into 4-micron thick slices and stained with H&E, Caspase-3, and Ki-67 to observe tissue morphology, cell proliferation, and apoptosis.

## 2.9 Statistical analysis

Statistical analyses were performed in GraphPad Prism. Differences in normalized tumor volumes and changes in animal weight were determined by one-way ANOVA. Where differences were detected, Tukey's post-test was used to test for significance between groups. The default significance level was set at  $\alpha = 0.05$  for all statistical tests.  $P < 0.05$  were considered statistically significant (\*  $P < 0.05$ , \*\*  $P < 0.01$ , \*\*\*  $P < 0.001$ ). Data was reported as mean  $\pm$  standard error of the mean (SEM).

## 3. Results

### 3.1 HPMA copolymer synthesis and characterization

The HPMA copolymers were synthesized by free radical precipitation copolymerization to be greater than 45 kDa to have a size slightly above the renal threshold in order to have longer circulation times taking advantage of the EPR effect and allowing for targeting of HS receptors 8-12 hours post heating. Additionally, this was done to be consistent with the size of polymers used in previous accumulation studies<sup>9, 19, 20</sup>. The characteristics of the copolymers are summarized in Table 1.

### 3.2 In vitro efficacy of heat shock targeted and untargeted polymer-docetaxel conjugates with human prostate cancer cells

The ability of the HS-targeted and untargeted HPMA copolymer-DOC conjugates to inhibit the growth of DU145 human prostate cancer cells was first evaluated *in vitro*. In Figure 2, both targeted and untargeted conjugates were incubated with and without hyperthermia at varying concentrations of DOC. The  $IC_{50}$  for the HS-targeted copolymer conjugates and untargeted conjugates under normothermia were 14.9  $\pm$  3.5 and 16.2  $\pm$  4.6 nM respectively. When the copolymer conjugates were incubated with hyperthermia, the  $IC_{50}$  for targeted and untargeted copolymer conjugates shifted to 7.4  $\pm$  2.3 and 11.0  $\pm$  4.6 nM

respectively. It was expected that HS-targeting and hyperthermia would shift the IC<sub>50</sub> to a lower concentration.

### 3.3 In vivo MRgHIFU heating

Tumor temperatures were recorded during MRgHIFU hyperthermia treatments and the mean spatial temperature in the heated tumor was plotted as an average of the six mice treated in each group +/- one STD (Fig 3). Most groups were largely able to heat and maintain at a temperature of approximately 43°C for 500 seconds. However, a large amount of variability is observed for the tumors heated in the group treated with free DOC and may contribute to variability with tumor growth. Saline injected mice were heated and maintained at approximately 42°C +/- 2°C (Fig 3A), Free DOC injected mice were heated at approximately 41°C +/- 5°C (Fig 3B), Untargeted polymer-DOC heated to approximately 42°C +/- 2°C (Fig 3C), and HS-targeted polymer-DOC heated to approximately 44°C +/- 1°C (Fig 3D).

### 3.4 In vivo heat shock expression with and without HIFU hyperthermia

MRgHIFU hyperthermia was used to up-regulate the cell surface expression of GRP78 *in vivo* using DU145 human prostate cancer xenografts. After heat treatment to approximately 43°C for 500 seconds, the expression was observed 8 hours later by immunohistochemical analyses. As seen in Figure 4, tumors that were treated with MRgHIFU hyperthermia (Fig. 4B) showed much higher amounts of staining for GRP78 than did the tumors that were left untreated (Fig. 4A). This result indicates that HIFU hyperthermia by this method has the capability to up-regulate GRP78 receptors *in vivo*.

### 3.5 Tumor growth after combination therapy with HIFU

In previous work, it was shown that the combination of HS-targeted copolymer-DOC and mild hyperthermia via GNR-mediated PPTT led to significant tumor reduction versus controls<sup>11</sup>. Here, we examined if the same could be achieved via HIFU. Treatment groups of saline, free DOC, and untargeted polymer-DOC were used as controls and compared to HS-targeted polymer-DOC. In combination with hyperthermia, tumor growth in each group was slightly reduced (Fig 5C and 5D). As expected, saline alone had the largest growth (243% of the original tumor size) followed by hyperthermia alone (204%), free DOC alone (201%), free DOC with hyperthermia (159%), untargeted polymer-DOC (136%), HS-targeted polymer-DOC (119%), and untargeted polymer-DOC with hyperthermia (114%) (Fig 5). The only group to have a size reduction was the combination of HS-targeted polymer-DOC with HIFU hyperthermia having 96% of the original tumor volume 30 days after treatment (Fig 5). Additionally, there were no significant changes in animal weight over the 30-day experiment although the weights of the free DOC group decreased between day 20 and day 30.

### 3.6 Histological analyses of in vivo tumor efficacy

At the culmination of the 30-day monitoring period, each animal was sacrificed and the tumors were removed, collected, and analyzed by histology. Tissues were stained with H&E to observe tissue morphology, Caspase-3 to observe apoptosis, and Ki-67 to observe cell

proliferation. Each treatment group was compared with (+HT) and without HIFU hyperthermia (-HT). In Figure 6, control groups stained with H&E show a higher density of cells indicated by the darker color (green arrows). Additionally, this shows that the HS-targeted polymers with hyperthermia had the largest amount of necrotic regions (Fig 6). Tissues stained with Caspase-3 show cells that have synthesized Caspase-3 in cells undergoing apoptosis. This production is indicated by the brown coloration and is most prevalent in tumor tissues treated with combination of HS-targeted polymer-DOC and HIFU hyperthermia as compared to controls (yellow arrows, Fig 6). Lastly, tissues stained with Ki-67 show the nuclear protein that is present at low levels in quiescent cells but is increased in proliferating cells. Positively stained cells are stained brown as well. Again, combination of HS-targeted polymer-DOC conjugates and HIFU hyperthermia had the least amount of staining when compared to control groups (red arrows, Fig 6).

#### 4. Discussion

Previously we utilized GNR-mediated PPTT as a method to produce localized hyperthermia selectively in tumor tissue and enhance the delivery and efficacy of HS-targeted HPMA copolymer-drug conjugates<sup>9, 11</sup>. Compared to PPTT, HIFU has a greater penetration depth (20 cm vs 2 cm) and is completely non-invasive where PPTT requires a prior injection of nanoparticles delivered intravenously which then accumulates in tumor tissue by the EPR effect. After this injection, only a small fraction of the particles reach the tumor site leading to a large amount of off-target accumulation in other organs such as the liver and spleen<sup>12</sup>; long-term effects of this accumulation are unknown. Additionally, not all tumors exhibit the EPR effect and those that do can be variable<sup>5</sup>. PPTT is still in the early developmental stages whereas HIFU has recently been approved by the Food and Drug Administration (FDA) for the ablation of prostate cancer tissue<sup>21</sup>.

Mild hyperthermia has been applied to enhance the delivery of other nanomedicines including temperature-sensitive liposomal drug carriers<sup>22-25</sup>. However, when these liposomal systems are triggered, payload release occurs extracellularly at the tumor site. In this case the free drug can be subject to efflux pumps and hence reduced efficacy. Use of polymer-drug conjugates can be more advantageous since the mechanism of cellular uptake is endocytosis, reducing efflux pumps' removal of the drug in resistant cancer cases<sup>26</sup>. In addition, covalent attachment of the drug to the polymeric side chains and site-specific cleavage within the tumor cell reduce nonspecific leakage in the blood stream. Together, our results demonstrate that the use of HS-targeted polymer-drug conjugates and HIFU hyperthermia in a combination therapy has potential to further improve therapeutic efficacy when compared to other nanomedicine delivery systems for treating prostate cancer and other malignancies.

In this work, it is shown that the combination of HIFU hyperthermia with HS-targeted HPMA copolymer-DOC conjugates leads to improved therapeutic outcome against human prostate cancer xenografts in immune compromised nu/nu mice. Here, we used HS-targeted HPMA copolymer-DOC conjugates as they have shown a high potential for improved therapeutic efficacy in combination with mild hyperthermia<sup>11</sup>. The same HS-targeting peptides were also used for comparison keeping polymer characteristics similar<sup>11</sup>. When



comparing the HPMA copolymer conjugate characteristics of those synthesized here to those previously used with PPTT<sup>11</sup>, the  $M_w$  was slightly larger here being closer to 100 kDa than those used before having an  $M_w$  closer to 80 kDa<sup>11</sup>. The drug loading here was slightly less, approximately 4.5 wt% compared to 6.5 wt%, and peptide targeting was also slightly less, having approximately 14.5 wt% compared to 16 wt% used previously<sup>11</sup>. These characteristics could lead to lower amounts of binding and having less drug per polymer being internalized. The conjugates were tested *in vitro* to determine the  $IC_{50}$  and observe the effects of HS-targeting with and without hyperthermia. Without hyperthermia, the  $IC_{50}$  for untargeted and HS-targeted conjugates were similar but slightly improved for the HS-targeted group. Under mild hyperthermia conditions, the  $IC_{50}$  values of the conjugates shifted slightly to lower concentrations. Hyperthermia is known to sensitize the cells to chemotherapy and so it is expected that even the untargeted polymers would have a slight shift in  $IC_{50}$ .

*In vivo* it was expected that the use of hyperthermia via HIFU would upregulate the expression of GRP78 receptors on the cell surface. For the HS-targeting strategy to be effective, it was important to determine if HIFU hyperthermia had this capability. We previously established that this upregulation occurs between 8-12 hours after heating<sup>9</sup>. Therefore, in this work tumor sections were analyzed 8 hours after treatment with MRgHIFU hyperthermia. The results (Fig. 4) show that MRgHIFU hyperthermia does have this capability and is a viable method for use to enhance the efficacy of copolymer-DOC conjugates targeted toward these receptors. This is expected as HIFU has been shown to increase tumor temperature to hyperthermic levels and the up-regulation of these receptors is largely due to the increased stress on the cells from the heat accumulation in the tissues.

To demonstrate the improved efficacy of the HS-targeted conjugates in combination with HIFU hyperthermia, animals were treated with saline, free DOC, untargeted polymer-DOC, and HS-targeted polymer-DOC. HS-targeted polymer-DOC conjugates showed the greatest reduction in tumor growth versus the saline control without hyperthermia. These results are again similar to those that used PPTT to generate hyperthermia *in vivo*<sup>11</sup>. However, the extent of tumor reduction was not as great as seen with PPTT<sup>11</sup> (96% with HIFU vs 49% with PPTT on day 30). This could possibly be due to the slightly lower amounts of drug loading and targeting peptide content, or potential ablative effect of GNR to the cells surrounding the particles even under mild hyperthermia conditions. Both HIFU and GNR-mediated PPTT have their advantages and disadvantages for induction of hyperthermia. With PPTT, the selective accumulation in tumor tissue allows for easier application compared to other methods that require expensive imaging guidance techniques (e.g. MRI). Simply irradiating the tumor region along with healthy tissues will only create heating in the tumor tissue as this is where the GNRs reside. Although the superficial depth of penetration would not allow the treatment of deep seated tumors, it could be applied to superficial or easily accessible tumors. Laser irradiation can easily be altered by adjusting the laser power and in turn tune the temperature without much hassle. With MRgHIFU, obtaining uniform heating at the desired temperature may require several adjustments at once.

In clinical applications that use HIFU ablation or surgical resection to treat prostate cancer, it may become difficult to ablate or remove cancerous tissues located near important healthy

structures including the urethra. The cancer may have begun to invade the surrounding tissues becoming difficult to ablate or surgically remove because of proximity to these important structures. Therefore, the combination therapy performed here may have the capability to completely destroy those areas that are difficult to treat otherwise by HIFU ablation alone. Incomplete resection or ablation procedures may result in continued cancer growth that may lead to the development of metastatic prostate cancer. If this development occurs, the 5-year survival dramatically drops from near 100% to about 28% with a median survival of about 4 years<sup>27</sup>. Therefore, treatment modalities must ensure that these advanced localized cancers are completely eliminated and not allowed to further progress. In addition to the survival benefit, the use of this proposed combination therapy will decrease complications of incontinence and erectile dysfunction as more precaution can be taken leading to a higher quality of life after the cancer is eradicated.

As HIFU begins to increasingly be used in the clinic for the treatment of other cancers (breast<sup>18, 28</sup>, liver<sup>29, 30</sup>, pancreas<sup>31, 32</sup>), so does the potential capability of the combination therapy shown here. HS-targeting can be used in cancers of the liver and breast where the same HS receptors can be targeted<sup>33, 34</sup>. Therefore, this treatment option can potentially be applied to a broad range of malignancies.

## Acknowledgments

Funding: The authors acknowledge financial support from the National Institutes of Health awarded to the Huntsman Cancer Institute (P30 CA042014) and Department of Radiology and Imaging Sciences (F32 HD085685). Support from the Experimental Therapeutics Program of the Huntsman Cancer Institute is also acknowledged.

## References

1. Duncan R, Vicent MJ. Polymer therapeutics-prospects for 21st century: The end of the beginning. *Advanced Drug Delivery Reviews*. 2013; 65:60–70. [PubMed: 22981753]
2. Maeda H. Macromolecular therapeutics in cancer treatment: The EPR effect and beyond. *Journal of Controlled Release*. 2012; 164:138–144. [PubMed: 22595146]
3. Working PK, Newman MS, Huang SK, Mayhew E, Vaage J, Lasic DD. Pharmacokinetics, Biodistribution and Therapeutic Efficacy of Doxorubicin Encapsulated in Stealth<sup>®</sup> Liposomes (Doxil<sup>®</sup>). *Journal of Liposome Research*. 1994; 4:667–687.
4. Bae YH, Mrsny RJ, Park K. *Cancer Targeted Drug Delivery: An Elusive Dream*. Springer Science & Business Media. 2013
5. Chauhan VP, Stylianopoulos T, Boucher Y, Jain RK. Delivery of Molecular and Nanoscale Medicine to Tumors: Transport Barriers and Strategies. *Annual Review of Chemical and Biomolecular Engineering*. 2011; 2:281–298.
6. Maeda H, Nakamura H, Fang J. The EPR effect for macromolecular drug delivery to solid tumors: Improvement of tumor uptake, lowering of systemic toxicity, and distinct tumor imaging in vivo. *Advanced Drug Delivery Reviews*. 2013; 65:71–79. [PubMed: 23088862]
7. Song CW. Effect of Local Hyperthermia on Blood Flow and Microenvironment: A Review. *Cancer Research*. 1984; 44:4721s–4730s. [PubMed: 6467226]
8. Frazier N, Ghandehari H. Hyperthermia approaches for enhanced delivery of nanomedicines to solid tumors. *Biotechnology and Bioengineering*. 2015; 112:1967–1983. [PubMed: 25995079]
9. Gormley AJ, Larson N, Sadekar S, Robinson R, Ray A, Ghandehari H. Guided delivery of polymer therapeutics using plasmonic photothermal therapy. *Nano Today*. 2012; 7:158–167. [PubMed: 22737178]
10. Sato, M., Yao, VJ., Arap, W., Pasqualini, R. 5 - GRP78 Signaling Hub: A Receptor for Targeted Tumor Therapy. In: Renata, P., editor. *Advances in Genetics*. Academic Press; 2010. p. 97-114.

11. Larson N, Gormley A, Frazier N, Ghandehari H. Synergistic enhancement of cancer therapy using a combination of heat shock protein targeted HPMA copolymer–drug conjugates and gold nanorod induced hyperthermia. *Journal of Controlled Release*. 2013; 170:41–50. [PubMed: 23602864]
12. Gormley AJ, Malugin A, Ray A, Robinson R, Ghandehari H. Biological evaluation of RGDfK-gold nanorod conjugates for prostate cancer treatment. *Journal of Drug Targeting*. 2011; 19:915–924. [PubMed: 22082105]
13. Gormley AJ, Greish K, Ray A, Robinson R, Gustafson JA, Ghandehari H. Gold nanorod mediated plasmonic photothermal therapy: A tool to enhance macromolecular delivery. *International Journal of Pharmaceutics*. 2011; 415:315–318. [PubMed: 21669265]
14. Christensen, DA. *Ultrasonic Bioinstrumentation*. New York: Wiley; 1988.
15. Frazier N, Payne A, de Bever J, Dillon C, Subrahmanyam N, Panda A, Ghandehari H. High Intensity Focused Ultrasound Hyperthermia for Enhanced Macromolecular Delivery. *Journal of Controlled Release*. 2016; 241:186–193. [PubMed: 27686583]
16. Strohalm J, Kopeček J. Poly[N-(2-hydroxypropyl)methacrylamide]. IV. Heterogeneous polymerization. *Die Angewandte Makromolekulare Chemie*. 1978; 70:109–118.
17. Ray A, Larson N, Pike DB, Gruner M, Naik S, Bauer H, Malugin A, Greish K, Ghandehari H. Comparison of Active and Passive Targeting of Docetaxel for Prostate Cancer Therapy by HPMA Copolymer–RGDfK. *Conjugates Molecular Pharmaceutics*. 2011; 8:1090–1099. [PubMed: 21599008]
18. Deckers R, Merckel LG, Denis de Senneville B, Schubert G, Köhler M, Knuttel FM, Mali WRPThM, Moonen CTW, van den Bosch MAAJ, Bartels LW. Performance analysis of a dedicated breast MR-HIFU system for tumor ablation in breast cancer patients. *Physics in Medicine and Biology*. 2015; 60:5527. [PubMed: 26133986]
19. Gormley AJ, Larson N, Banisadr A, Robinson R, Frazier N, Ray A, Ghandehari H. Plasmonic photothermal therapy increases the tumor mass penetration of HPMA copolymers. *Journal of Controlled Release*. 2013; 166:130–138. [PubMed: 23262203]
20. Frazier N, Robinson R, Ray A, Ghandehari H. Effects of Heating Temperature and Duration by Gold Nanorod Mediated Plasmonic Photothermal Therapy on Copolymer Accumulation in Tumor Tissue. *Molecular Pharmaceutics*. 2015; 12:1605–1614. [PubMed: 25839226]
21. FDA Clears Focused Ultrasound System for Prostate Cancer Treatment. *Oncology Times*. 2015; 37:37.
22. Dicheva BM, ten Hagen TLM, Schipper D, Seynhaeve AL, van Rhooon GC, Eggermont AM, Koning GA. Targeted and heat-triggered doxorubicin delivery to tumors by dual targeted cationic thermosensitive liposomes. *Journal of Controlled Release*. 2014; 195:37–48. [PubMed: 25176578]
23. Li L, ten Hagen TLM, Haeri A, Soullie T, Scholten C, Seynhaeve AL, Eggermont AM, Koning GA. A novel two-step mild hyperthermia for advanced liposomal chemotherapy. *Journal of Controlled Release*. 2014; 174:202–208. [PubMed: 24269966]
24. Ta T, Bartolak-Suki E, Park E-J, Karrobi K, McDannold NJ, Porter TM. Localized delivery of doxorubicin in vivo from polymer-modified thermosensitive liposomes with MR-guided focused ultrasound-mediated heating. *Journal of Controlled Release*. 2014; 194:71–81. [PubMed: 25151982]
25. Ponce AM, Vujaskovic Z, Yuan F, Needham D, Dewhirst MW. Hyperthermia mediated liposomal drug delivery. *International Journal of Hyperthermia*. 2006; 22:205–213. [PubMed: 16754340]
26. Minko T, Kopeček P, Kopeček J. Efficacy of the chemotherapeutic action of HPMA copolymer-bound doxorubicin in a solid tumor model of ovarian carcinoma. *International Journal of Cancer*. 2000; 86:108–117. [PubMed: 10728603]
27. *Cancer Facts and Figures 2015*. Atlanta, Ga: American Cancer Society; 2015.
28. Wu F, ter Haar G, Chen WR. High-intensity focused ultrasound ablation of breast cancer. *Expert Review of Anticancer Therapy*. 2007; 7:823–831. [PubMed: 17555392]
29. Wijlemans JW, de Greef M, Schubert G, Bartels LW, Moonen CT, van den Bosch MA, Ries MA. Clinically Feasible Treatment Protocol for Magnetic Resonance-Guided High-Intensity Focused Ultrasound Ablation in the Liver. *Investigational Radiology*. 2015; 50:24–31.

30. Zavaglia C, Mancuso A, Foschi A, Rampoldi A. High-intensity focused ultrasound (HIFU) for the treatment of hepatocellular carcinoma: is it time to abandon standard ablative percutaneous treatments? *Hepatobiliary Surgery and Nutrition*. 2013; 2:184–187. [PubMed: 24570943]
31. Khokhlova TD, Hwang JH. HIFU for palliative treatment of pancreatic cancer. *Journal of Gastrointestinal Oncology*. Sep.2011 2(3)
32. Jang HJ, Lee J-Y, Lee D-H, Kim W-H, Hwang JH. Current and Future Clinical Applications of High-Intensity Focused Ultrasound (HIFU) for Pancreatic Cancer. *Gut and Liver*. 2010; 4:S57–S61. [PubMed: 21103296]
33. Cook KL, Clarke PAG, Clarke R. Targeting GRP78 and antiestrogen resistance in breast cancer. *Future Medicinal Chemistry*. 2013; 5:1047–1057. [PubMed: 23734687]
34. Lee AS. Glucose regulated proteins in cancer: molecular mechanisms and therapeutic potential. *Nature reviews Cancer*. 2014; 14:263–276. [PubMed: 24658275]

## Abbreviations

<b>AIBN</b>	Azobisisobutyronitrile
<b>ANOVA</b>	Analysis of variance
<b>DOC</b>	Docetaxel
<b>EBD</b>	Evans blue dye
<b>ESI/MS</b>	Electrospray ionization mass spectroscopy
<b>EPR</b>	Enhanced permeability and retention
<b>FBS</b>	Fetal bovine serum
<b>FDA</b>	Food and Drug Administration
<b>Gd</b>	Gadolinium
<b>GNR</b>	Gold nanorod
<b>GRP78</b>	Glucose-regulated protein-78
<b>HIFU</b>	High intensity focused ultrasound
<b>HPMA</b>	<i>N</i> -(2-hydroxypropyl)methacrylamide
<b>IC<sub>50</sub></b>	Inhibitory concentration of 50%
<b>ID</b>	Injected dose
<b>MA-GFLG-DOC</b>	<i>N</i> -methacryloyl-glycylphenylalanylleucylglycine-docetaxel
<b>MA-GG-TT</b>	<i>N</i> -methacryloylglycylglycyl-2-thiazolidine-2-thione
<b>MFH</b>	Magnetic fluid hyperthermia
<b>M<sub>n</sub></b>	Number average molecular weight
<b>MRI</b>	Magnetic resonance imaging
<b>M<sub>w</sub></b>	Weight average molecular weight

<b><math>M_w/M_n</math></b>	Polydispersity index
<b>MRgHIFU</b>	Magnetic resonance imaging-guided HIFU
<b>PBS</b>	Phosphate buffered saline
<b>PDI</b>	Polydispersity index
<b>PPTT</b>	Plasmonic photothermal therapy
<b>RFA</b>	Radiofrequency ablation
<b>SEC</b>	Size exclusion chromatography
<b>Seg-EPI</b>	Segmented-echo planar imaging
<b>TE</b>	Echo time
<b>TR</b>	Repetition time

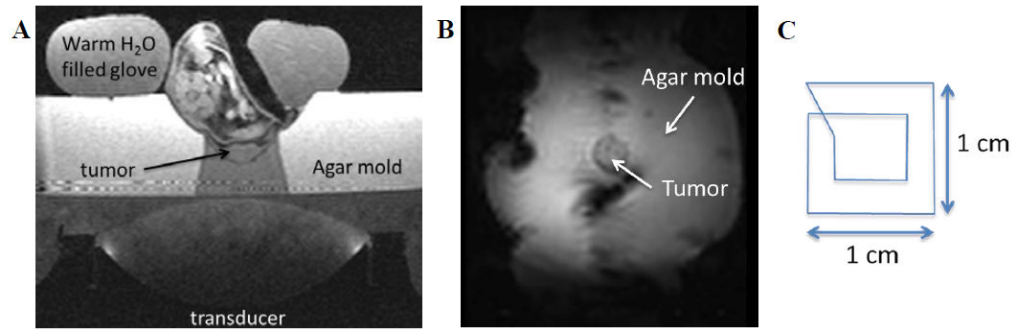


**Figure 1.** Schematic of *in vivo* heating setup. A) Axial image of small animal MRgHIFU system used to heat tumor tissue *in vivo*. B) Coronal image of *in vivo* setup with the treated tumor surrounded by the agar mold. C) Heating pattern for producing uniform heating.

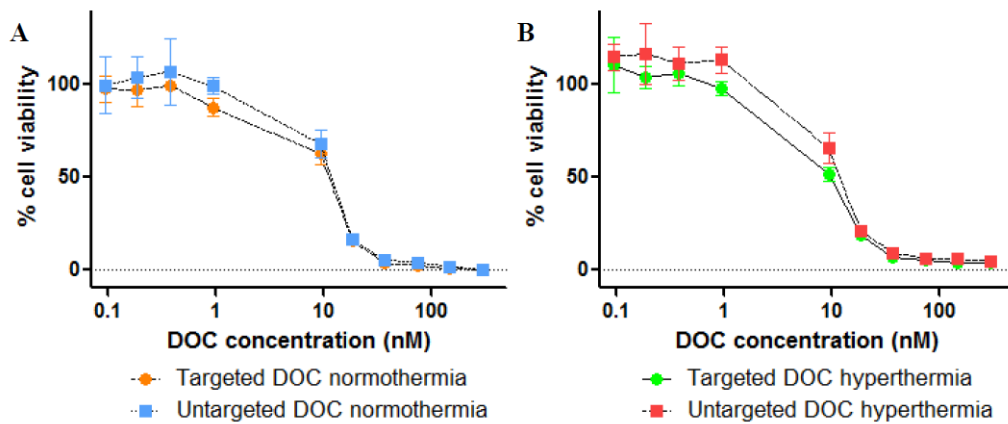


**Figure 2.** *In vitro* efficacy of heat shock targeted and untargeted polymer-docetaxel conjugates incubated in combination with A) normothermia (37°C for 72 hours) or with B) hyperthermia (43 °C for 30 minutes followed by 37°C for 71.5 hours). Data is expressed as mean +/- STD with n=4 for each sample and concentration. No significant differences in IC<sub>50</sub> are observed.

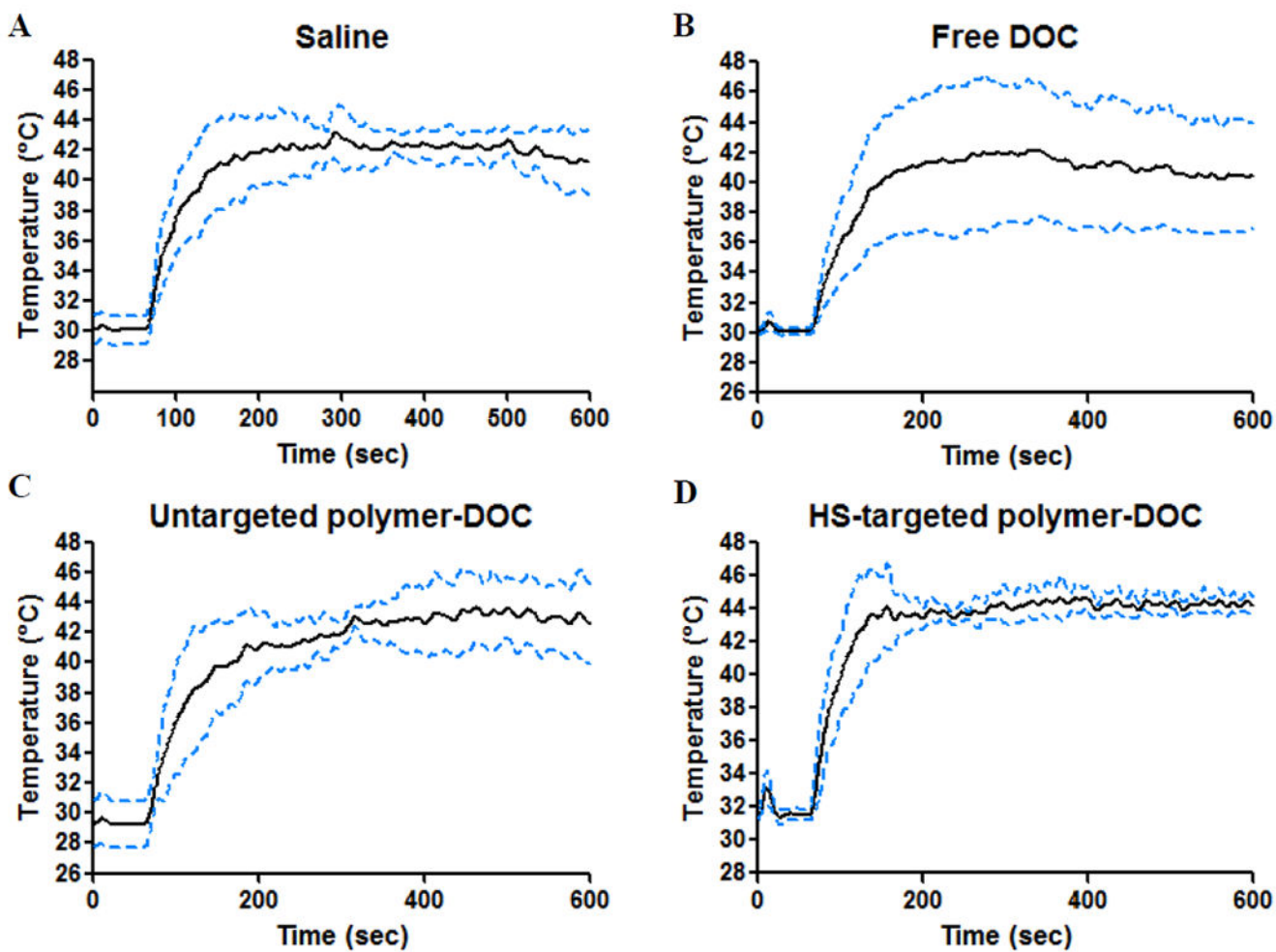


**Figure 3.**  
*In vivo* MRgHIFU heating temperature profiles (average  $\pm$  STD) of individual treatment groups: A) Saline, B) Free docetaxel, C) Untargeted polymer-docetaxel, and D) Heat shock-targeted polymer-docetaxel. For each treatment group  $n=6$ .



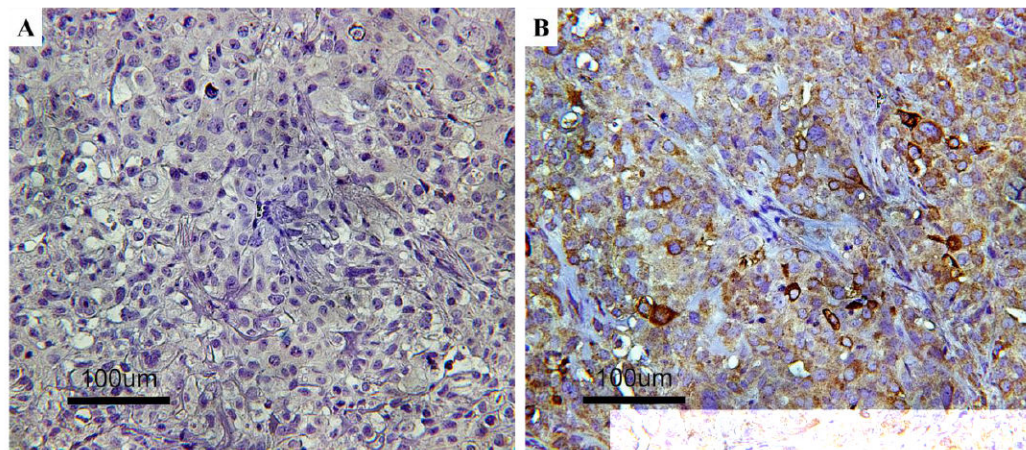


**Figure 4.** (A) Control tumor tissue stained for expression of GRP78 cell receptors. (B) HIFU hyperthermia treated tumor tissue stained for GRP78 cell receptors shown by the red-brown color.

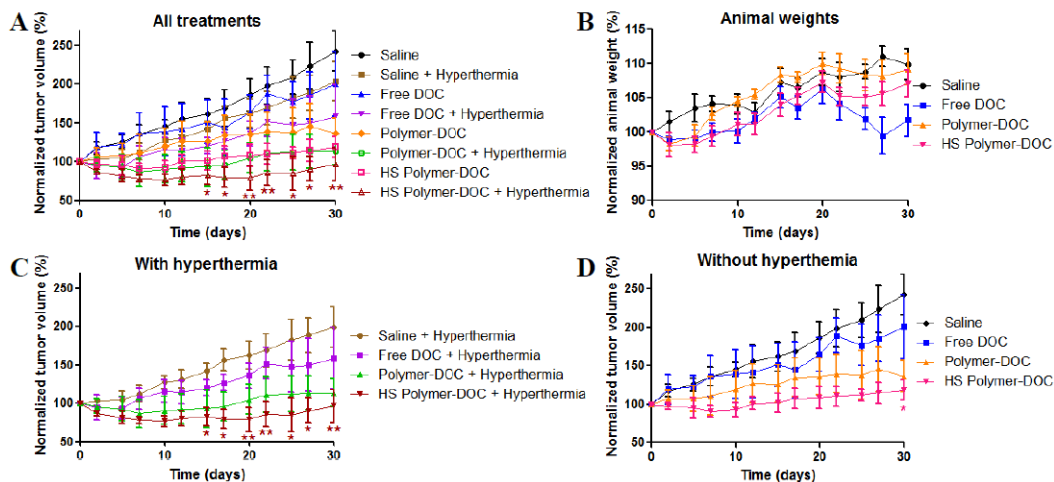


**Figure 5.** *In vivo* efficacy of HIFU hyperthermia and heat shock-targeted polymer-docetaxel. A) Tumor volume over 30 days when injected with saline, free docetaxel (free DOC), untargeted polymer-docetaxel (polymer-DOC), or heat shock-targeted polymer-docetaxel (HS polymer-DOC) with and without HIFU hyperthermia. B) Animal weights when injected with saline, free DOC, polymer-DOC, or HS polymer-DOC. C) Treatment groups with hyperthermia. D) Treatment groups without hyperthermia. For each treatment group n=6. \* And \*\* indicate statistical significance compared to saline control.

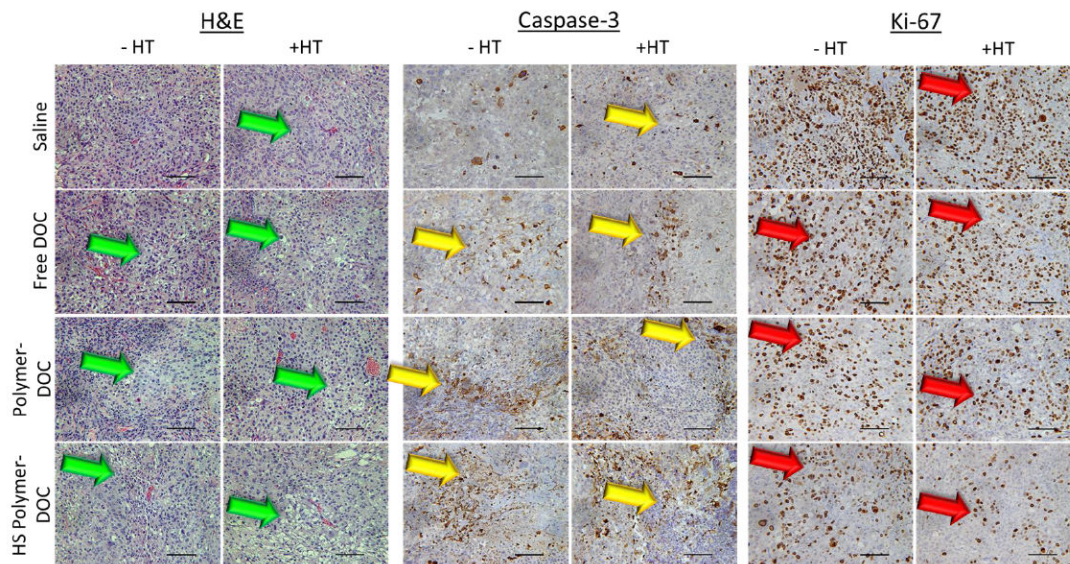


**Figure 6.** Histological analyses of tumor tissue treated with saline, free docetaxel (free DOC), untargeted polymer-docetaxel (polymer-DOC), or heat shock-targeted polymer-docetaxel (HS polymer-DOC) with (+HT) and without HIFU hyperthermia (-HT). Tissues were stained with H&E (tissue morphology), Caspase-3 (apoptosis), and Ki-67 (cell proliferation). Green arrows indicate necrotic regions, yellow arrows indicate cells undergoing apoptosis, and red arrows indicate cells undergoing proliferation. 20x magnification. Scale bars =100  $\mu$ m.

**Table 1**

HPMA copolymer characteristics.

Sample	M <sub>W</sub> (kDa)	PDI	Drug content (wt%)	Targeting peptide content (wt%)
Targeted copolymer-DOC	97	1.9	4.6 +/- 0.46	14.5 +/- 0.39
Untargeted copolymer-DOC	94	1.9	4.7 +/- 0.37	13.9 +/- 1.16

Author Manuscript

Author Manuscript

Author Manuscript

Author Manuscript